

# Design Of An Anisokinetic Probe For Sampling Radioactive Particles From Ducts Of Nuclear Facilities

Author P. Geraldini<sup>1</sup>

<sup>1</sup>Sogin Spa

Via Marsala 51C, 00185 Rome – Italy, geraldini@sogin.it

**Abstract:** The International Standard ISO 2889 focuses on monitoring the activity concentrations and activity releases of radioactive substances in air in ducts and stacks of nuclear facilities. It also provides performance-based criteria for the design and use of air-sampling equipment, including probes, transport lines, sample collectors, sample monitoring instruments and gas flow measuring methods.

A shrouded nozzle sampling probe (McFarland et al., 1989) is basically a nozzle fitted with a flow decelerator. It is less susceptible to off-design sampling conditions (e.g. off-angle flow direction, flow turbulence, changes in sampling flow rate or changes in the free-stream velocity) and it has lower wall losses than an unshrouded nozzle (Chandra and McFarland, 1995).

A sampling nozzle should have well-defined geometrical and aerodynamical features and the transmission ratio (ratio of the aerosol particle concentration at the nozzle outlet to that in the free stream) must be within the range of 0,80 to 1,30 for an aerosol with a particle aerodynamic diameter of 10  $\mu\text{m}$ .

The aim of this study is to design a new concept of shrouded probe that meets the ISO 2889 requirements and it is suitable for small-ducts installation. In order to reduce the construction costs they have been considered standard stainless steel welding fittings manufactured according to ASME/ANSI specifications.

In particular, with the numerical simulations, they have been firstly evaluated the capabilities of the numerical model to reproduce the available experimental data for a commercial shrouded probe and secondly they have been investigated the performances of the new concept design.

The 3D simulations have been performed with COMSOL Multiphysics® version 5.1 (Heat Transfer and Particle Tracing Modules). The simulations are based on the following segregated steps: fluid flow study (single-phase incompressible turbulent k- $\epsilon$  wall function) and time dependent transport of particles (Lagrangian

approach). The trajectories of particles in the flow field are simulated including such effects as inertia, drag, gravity and turbulent diffusion. Computations are carried out for free stream velocities in the range of 2 to 25 m/s and for particle size of 5, 10 and 15  $\mu\text{m}$  aerodynamic equivalent diameter.

The results presented in this study confirm the capability of COMSOL Multiphysics® as a multiphysics simulation tool. The development of this work has allowed us to obtain useful indications for the design of the new concept probe.

**Keywords:** CFD, particle tracing, nuclear, shrouded probe.

## 1. Introduction

The International Standard ISO 2889 [1] focuses on monitoring the activity concentrations and activity releases of radioactive substances in air in ducts and stacks of nuclear facilities and sets the performance criteria and recommendations required for obtaining valid measurements. It also provides performance-based criteria for the design and use of air-sampling equipment, including probes, transport lines, sample collectors, sample monitoring instruments and gas flow measuring methods. The recommendations are aimed at sampling that is conducted for worker and environmental protection, regulatory compliance and system control.

In the nuclear industry, the standard protocol for sampling radioactive particles from a moving gas stream involves the use of isokinetic probes (condition that prevails when the velocity of air at the inlet plane of a nozzle is equal to the velocity of undisturbed air in a stack or duct at the point where the nozzle inlet is located [1]). Under both isokinetic and anisokinetic conditions, these probes create substantial errors in quantifying the concentration of aerosol particles in the free stream. The isokinetic errors are due to the loss of particles to internal walls of

measure equipment. For reducing the sampling errors McFarland et al. [2] developed a new device, a shrouded probe. The typical geometry of a shrouded probe is shown in Figure 1. By employing an aerodynamic shroud around a sampling probe, the flow entering the probe can be decelerated relative to the free stream and the probe can be operated anisokinetically relative to the free stream and still produce only small sampling errors. This offers potential to sample at a constant flow rate in a variable velocity flow stream. It is less susceptible to off-design sampling conditions (e.g. off-angle flow direction, flow turbulence, changes in sampling flow rate or changes in the free-stream velocity) and it has lower wall losses than an unshrouded nozzle [4].

The aim of this study is to design a new concept of shrouded probe that meets the ISO 2889 requirements and it is suitable for small-ducts installation (from 200 to 400 mm equivalent diameter). In order to reduce the construction costs they have been considered standard stainless steel welding fittings manufactured according to ASME/ANSI specifications.

In particular, with the numerical simulations, they have been firstly evaluated the capabilities of the numerical model to reproduce the available experimental data for a commercial shrouded probe and secondly they have been investigated the performances of the new concept design.

## 2. ISO 2889 requirements

According with ISO 2889, a sampling nozzle should have well-defined geometrical and aerodynamical features and the transmission ratio (ratio of the aerosol particle concentration at the nozzle outlet  $C_{pout}$  to that in the free stream  $C_0$ ) must be within the range of 0,80 to 1,30 for an aerosol with a particle aerodynamic equivalent diameter AED of 10  $\mu\text{m}$ . The transmission ratio  $\tau$  is expressed by the following formula:

$$\tau = \frac{C_{pout}}{C_0} = \left( \frac{C_{pin}}{C_0} \right) (1 - F_{wl}) \quad (1)$$

$$= A(1 - F_{wl})$$

where  $A$  is the aspiration ratio defined as the ratio of the mean particle concentration at the inlet plane of the probe ( $C_{pin}$ ) to that in the free stream ( $C_0$ ) and  $F_{wl}$  is the fraction of particles deposited on the internal surface of the probe respect to the

particles entered into the probe. Following the approach described by Gong [3] the previous equation can be rewritten as:

$$\tau = \left( \frac{N_{pr}}{N_0} \right) \left( \frac{U_0}{U_{pr}} \right) \left( \frac{A_0}{A_{pr}} \right) \left( 1 - \frac{N_{wl}}{N_{pr}} \right) \quad (2)$$

$$= \left( \frac{N_{prout}}{N_0} \right) \left( \frac{U_0}{U_{pr}} \right) \left( \frac{A_0}{A_{pr}} \right)$$

where  $N_0$  is the number of particles uniformly distributed in the cross-sectional area  $A_0$  in the free stream,  $N_{pr}$  is the number of particles passing through the cross-sectional area  $A_{pr}$  of the probe inlet,  $N_{prout}$  is the number of particles that reached the sampling section (see Figure 3 and Figure 7),  $U_0$  is the free stream mean velocity,  $U_{pr}$  is the mean velocity at the probe inlet and  $N_{wl}$  is the number of particles deposited on the internal surface of the probe. During the simulations, in order to obtain a correct value for  $A$ , the area  $A_0$  should be specified to be large enough such that all the particles that can pass through the inlet cross section of the probe are initially located within  $A_0$ . A sufficient number of particles  $N_0$  is also required to get values of the aspiration ratio, the wall loss, and the transmission ratio that are independent of the number of particles distributed in the area  $A_0$ .

## 3. Numerical model

In this section they are presented the geometrical and mechanical features of the probes, the governing equations of the numerical modeling and their boundary conditions.

### 3.1 Geometrical and mechanical stack's design

The next Figure 1 shows the commercial probe characteristics. The inlet diameter of the probe is 15 mm, which provides a mean velocity at the probe inlet plane  $U_{pr}$  of 5 m/s (with a sampling flow rate fixed at 56.6 l/min). The probe body is gradually expanded for a transition to a 45 mm external diameter aerosol transport line. The inside and outside diameters of the shroud are 52 and 58 mm, respectively. The inlet is located 90 mm from the shroud entrance plane. The waistline on the outside surface of the probe is expanded to provide a blockage of the cross-sectional area between the shroud and the probe; for the case of the commercial probe, the open area between the waistline of the probe and the

shroud is about 30% of the total shroud cross-sectional area. This blockage controls air flow through the shroud. The shroud is 176 mm long. Into the geometry they have been modelled the support fins (3 places) that connect the shroud to the probe.

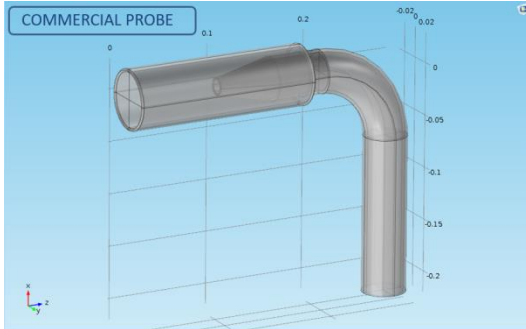


Figure 1. Geometry of commercial shrouded probe

The new concept shrouded probe is specifically designed for small-ducts installation (extraction ventilation ducts of hot-cells and other containments for which is not available commercial devices). In order to reduce the construction costs they have been considered standard stainless steel welding fittings manufactured according to ASME/ANSI specifications. The Figure 2 shows the new concept probe:

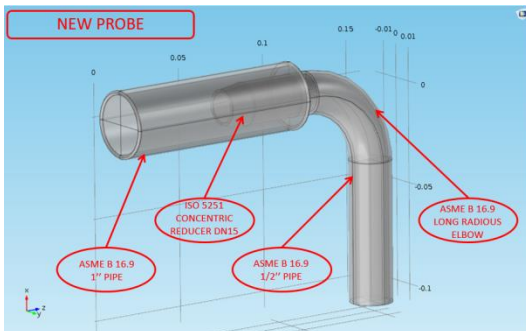


Figure 2. Geometry of new concept shrouded probe

The inlet diameter of the probe is 17.2 mm, which provides a mean velocity at the probe inlet plane  $U_{pr}$  of 2.5 m/s (with a sampling flow rate fixed at 37 l/min). The probe body is gradually expanded for a transition to a 21 mm external diameter aerosol transport line. The inside and outside diameters of the shroud are 30,1 and 33.4 mm, respectively. The inlet is located 50 mm from the shroud entrance plane. Regardless of

the sampling flowrate, they represent values of practical interest for sampling radioactive aerosol particles in the nuclear industry (Continuous Air Monitoring CAM working flow rate).

### 3.2 Governing equations

The governing equations used during the study are represented by partial differential equations derived by imposing the balance of mass (3) and momentum (4) within an infinitesimal element of volume. The last equation (5) represents the Newton's second law applied to each particle. The governing equations, for incompressible case are reported in tensorial form:

$$\nabla \cdot \mathbf{u} = 0 \quad (3)$$

$$\rho \frac{\partial \mathbf{u}}{\partial t} + \rho(\mathbf{u} \cdot \nabla)\mathbf{u} = \nabla \cdot [-p\mathbf{I} + \boldsymbol{\tau}] \quad (4)$$

$$\frac{d}{dt}(m_p \mathbf{v}) = \left(\frac{1}{\tau_p}\right) m_p (\mathbf{u}' - \mathbf{v}) + m_p \mathbf{g} \frac{(\rho_p - \rho)}{\rho_p} + \mathbf{F}_{brow} \quad (5)$$

where  $\mathbf{u}$  is the velocity vector,  $\mathbf{v}$  the particle velocity vector,  $\tau_p$  the particle velocity response time (the drag force takes into account the turbulent dispersion by means of  $\mathbf{u}'$  which is the turbulent velocity fluctuation),  $\mathbf{g}$  the gravity vector and  $\mathbf{F}_{brow}$  is the brownian force. The effect of the Saffman force on wall loss is negligible compared with the effects of turbulence diffusion [3]. For the other terms, please refer to Comsol Multiphysics Reference Manual.

### 3.3 Boundary conditions

For the first simulation step (fluid flow study), the following boundary conditions are applied: atmospheric pressure on the outlet domain section (suppress back flow option), logarithmic wall function on the probe walls, velocity inlet condition (normal flow velocity) on the entrance of the domain, velocity slip condition on the lateral domain boundaries and velocity outlet condition (normal outflow velocity) on the outlet sampling surface (see Figure 3).

The second simulation step concerns the particle tracing study. The particles are released from the surface  $A_0$  (see Figure 3) at initial time ( $t=0$ ), with uniform distribution along the section, and

initial velocity equal to the air local velocity field. The walls are treated by means freeze condition. According with the conclusions of Tian [7] the  $k-\epsilon$  turbulence model, which assumes isotropy, leads to high level of fluctuation perpendicular to the wall and to overprediction of nano and micro-scale particle deposition rates. This approach guarantees that the transmission ratio are conveniently underestimated respect to the reality. The other surfaces are modelled by means of freeze option. For more details about the numerical technique refer to § 4.

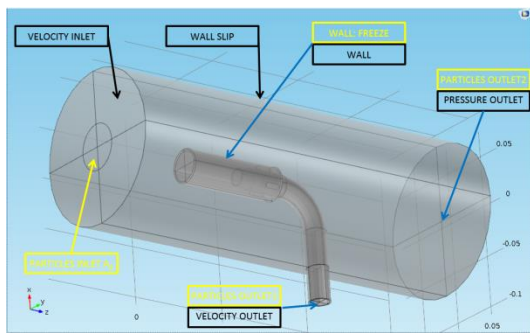


**Figure 3.** Boundary conditions detail for first (black) and second step (yellow) simulation

#### 4. Use of COMSOL Multiphysics

With the numerical simulations they have been firstly validated the capabilities of the numerical model to reproduce the available experimental data for a commercial shrouded probe (reported in [4] and [5]) and secondly they have been investigated the performances of the new concept design.

The 3D simulations have been performed with Comsol Multiphysics 5.1 – Heat Transfer and Particle Tracing Modules and they are based on the following steps: 1) stationary fluid flow study (single phase incompressible turbulent  $k-\epsilon$  closure model); 2) time dependent particle transport study (using the air velocity field obtained in the first study). The particle transport simulation is based on the “sparse flow” approach where the continuous phase affects the motion of the particles but not vice versa (one-way coupling). Computations are carried out for free stream velocities in the range of 2 to 25 m/s and for particle size of 5, 10 and 15  $\mu\text{m}$  aerodynamic equivalent diameter.

#### 4.1 Computational domains and meshes

The geometrical dimensions of the probes are reproduced in 1:1 scale (see Figure 1 and Figure 2). The flow study mesh consists of a tetrahedral network of about 520.000 elements with average element quality 0.56 (minimum quality 0.003) for both probes simulated. A finer mesh is used near the wall in order to guarantee sufficient small values of wall lift-off: as shown in Figure 4 it is larger than 11.06 only at some locations near the probe inlet section and along the impingement zone of sampling pipe. The mesh used for the particle tracing study is finer than the previous one to yield sufficiently accurate results and for a reasonably short simulation time (and 6 hours for 5 micron aerodynamic diameter particle study on a workstation Intel Xeon CPU @ 2.40 GHz, 64 GB RAM). In particular the particle study mesh is represented by a tetrahedral network of about 1.350.000 elements with average element quality 0.62 (minimum quality 0.007) for both probes simulated.

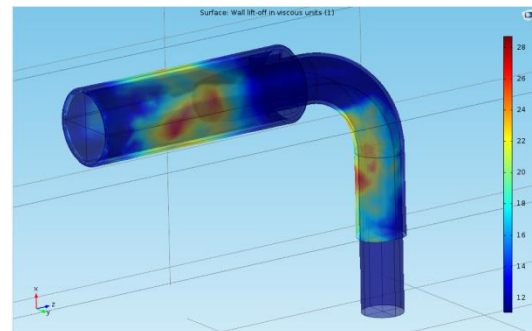


**Figure 4.** Wall lift-off in viscous unit for the highest free stream velocity

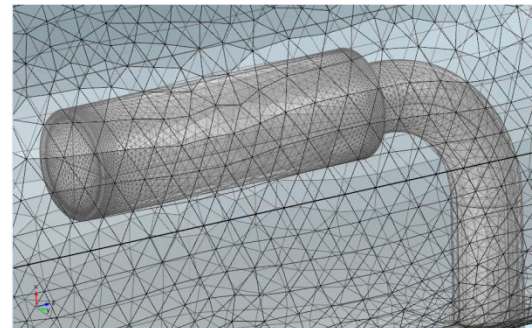


**Figure 5.** Mesh detail for the particle tracing step

#### 4.2 Solver set-up for fluid flow study

The stationary fluid flow study is used to obtain the velocity field inside the probes. The physics

selected is single phase turbulent flow k- $\epsilon$  formulation as closure model (wall function). As described in § 3.2 the flow is considered incompressible. The direct, MUMPS, segregated solver configuration is used during the simulation. The solution is considered to be converged when the residual values fell below less than  $10^{-6}$ .

#### 4.3 Solver set-up for particle transport study

The time dependent particle transport study is used to obtain the aerosol concentration profile along the outlet sampling surface (i.e. the number of particles  $N_{prouit}$  that reach the sampling surface). The Transient Newtonian formulation is employed with Standard Drag Correlations law implementation. As described in § 3.2 the forces considered are the drag, the gravity and Brownian ones. They have been performed different computational studies that represent the combinations of different external free velocity and three aerodynamic diameters. The transient simulations are extended for a simulation time long enough to allow the adhesion of particles to the stick surfaces or to reach the outlet section. The transmission ratio of the shrouded probes has been evaluated statistically by tracking a large number of particles. Based on Gong study [3] 10.000 particles were found to be sufficient to give results independent of the number of particles. The direct, MUMPS, fully-coupled solver configuration is used during the simulation. The solution is considered to be converged when the residual values fell below less than  $10^{-8}$ .

### 5. Results

The paragraph 5.1 shows the capabilities of the numerical model to reproduce the available experimental data for a commercial shrouded probe whereas in § 5.2 are summarized the performances of the new concept design.

#### 5.1 Commercial probe

With reference to Figure 6 the multislice plot shows the velocity magnitude field inside the shroud and inside the probe for the lower external free stream velocity. The particle trajectories for the maximum air stream velocity studied (25 m/s) for 5  $\mu\text{m}$  aerodynamic diameter are shown in Figure 7. Figure 8 shows the predicted variation of the transmission ratio with particle size and external flow velocity.

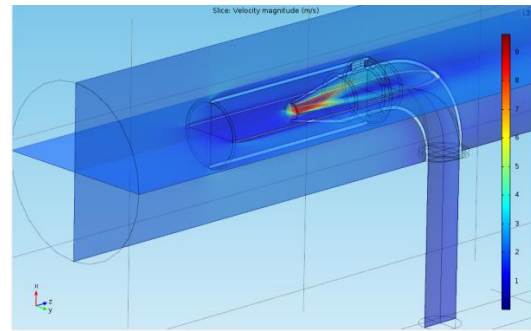


**Figure 6.** Multislice plot of velocity magnitude field for commercial probe at minimum air stream velocity (2 m/s)

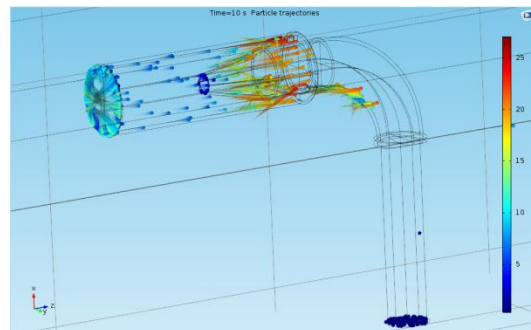


**Figure 7.** Particle trajectories (comet tail diagram) for 5  $\mu\text{m}$  aerodynamic diameter and maximum air stream velocity (25 m/s)

Experimental results are also shown in the same figure. The numerical results are given for free stream velocities in the range of 2 to 25 m/s and for particle size of 10  $\mu\text{m}$  aerodynamic diameter. It is evident that the numerically predicted transmission ratios compare well with the experimentally determined values. The maximum difference is less than 10%, probably due to conservative hypothesis of stick walls.

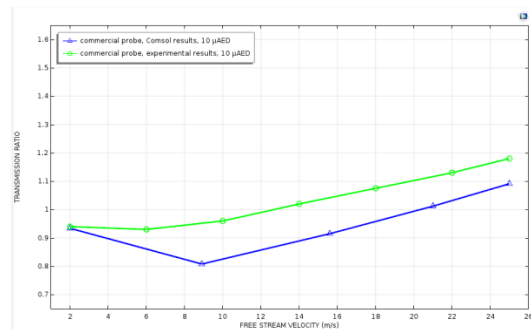


**Figure 8.** Comparison of transmission ratio for commercial probe (numerical and experimental)

## 5.2 New concept probe

With reference to Figure 9 the multislice plot shows the velocity magnitude field inside the shroud and inside the probe for lower free stream velocity. The particle trajectories for the maximum air stream velocity studied (25 m/s) for 5  $\mu\text{m}$  aerodynamic diameter are shown in Figure 10. Figure 11, Figure 12 and Figure 13 and show the predicted variation of the transmission ratio with particle size and external flow velocity compared to the commercial probe.

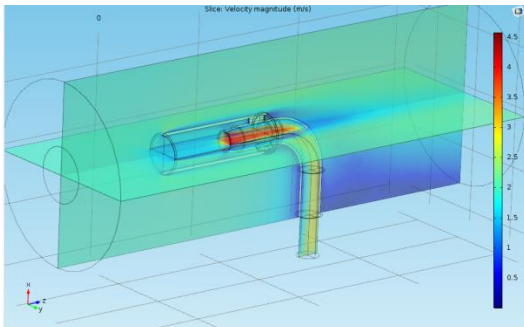


**Figure 9.** Multislice plot of velocity magnitude field for new concept probe at minimum air stream velocity (2 m/s)

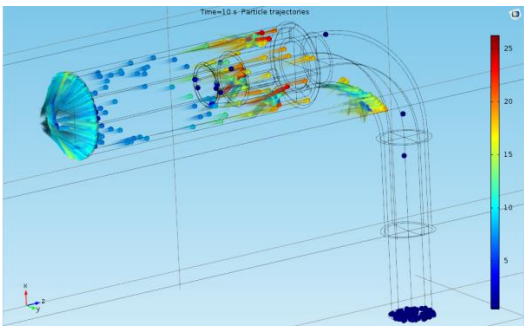


**Figure 10.** Particle trajectories (comet tail diagram) for 5 micron aerodynamic diameter and maximum air stream velocity (25 m/s)

From the Figure 8, Figure 11, Figure 12 and Figure 13 can be seen that under conditions in which the free stream velocity is large, the shroud probes both allow a lower velocity sample to be presented to the inlet and permits a larger probe diameter to be employed. Although the velocity in the shroud is anisokinetic relative to the free stream velocity, the large diameter of the shroud reduces the magnitude of the inertial enrichment or depletion of aerosol concentration that is the usual consequence of anisokinetic sampling, especially for the commercial probe.

The new concept probe seems to be less flexible than the other one and the variation of transmission ratio with the velocity is more evident.

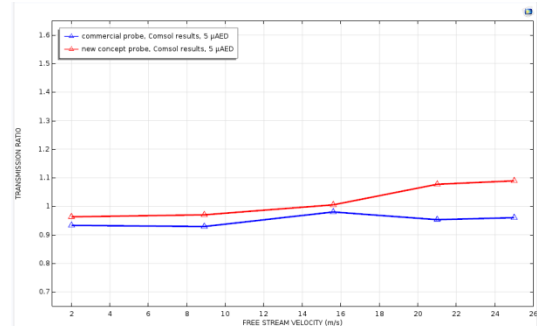


**Figure 11.** Comparison of transmission ratio for commercial probe and new concept probe for 5  $\mu\text{m}$  aerodynamic diameter

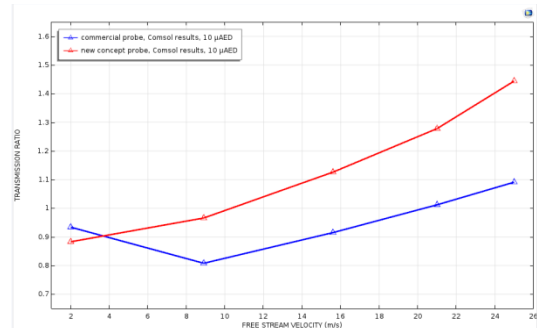


**Figure 12.** Comparison of transmission ratio for commercial probe and new concept probe for 10  $\mu\text{m}$  aerodynamic diameter

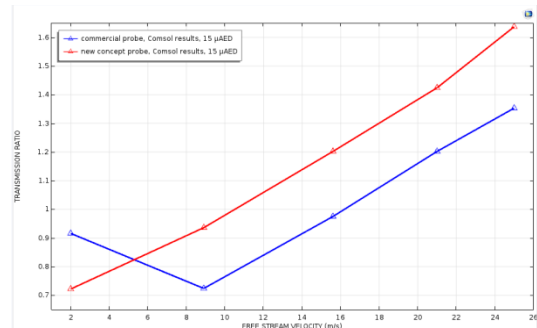


**Figure 13.** Comparison of transmission ratio for commercial probe and new concept probe for 15  $\mu\text{m}$  aerodynamic diameter

The transmission ratio of a shrouded probes increases with both free stream velocity and particle size. The transmission ratio of new concept probe is slightly higher than the commercial one and a sampling flow rate

optimization study can be performed in order to modify the behavior of the probe with a velocity.

## **6. Conclusions**

The results presented in this study confirm the capability of COMSOL Multiphysics® as a multiphysics simulation tool. The study allowed us to design a new concept of shrouded probe that meets the ISO 2889 requirements and it is suitable for small-ducts installation and to reduce the construction costs considering standard stainless steel welding fittings manufactured according to ASME/ANSI specifications.

## **7. References**

- [1]. ISO 2889, Sampling airborne radioactive materials from the stacks and ducts of nuclear facilities, second edition 2010;
- [2]. A. R. McFarland, A Shrouded Aerosol Sampling Probe, *Environ. Sci. Technol.*, Vol.23, No. 12,1989;
- [3]. H. Gong, Numerical Prediction of the Performance of the Shrouded Probe Sampling in TurbulentFlow, *Aerosol Sc. Tech.* 1993;
- [4]. S. Chandra, A. R. McFarland, Comparison of Aerosol Sampling with Shrouded and Unshrouded Probes, *American Industrial Hygiene Association Journal* 1995;
- [5]. H. Gong, A Predictive Model for Aerosol Transmission Through a Shrouded Probe, *Environ. Sci.Technol.*, Vol. 30, No. 11, 1996;
- [6]. S. Chandra, Shrouded Probe Performance: Variable Flow Operation and Effect of the Free Stream Turbulence, *Aer. Sc. Tech.* 1997;
- [7]. L. Tian, Particle deposition in turbulent duct flows—comparisons of different model predictions,*Aerosol Science* 38, 2007;
- [8]. S. Parker, Towards quantitative prediction of aerosol deposition from turbulent flows, *Aerosol Science* 39, 2008.